



## OPEN ACCESS

## EDITED BY

Chao Zeng,  
Jiangxi Normal University, China

## REVIEWED BY

Xiaohui Ren,  
Wuhan University of Science and Technology,  
China  
István Székely,  
Babeş-Bolyai University, Romania  
Chunhui Dai,  
East China University of Technology, China  
Jianhua Zhang,  
Wuhan Textile University, China

## \*CORRESPONDENCE

Javed Ali Khan,  
✉ javedkhan@awkum.edu.pk,  
✉ khanjaved2381@gmail.com  
Muhammad Ateeq,  
✉ m.ateeq@awkum.edu.pk

RECEIVED 19 July 2024

ACCEPTED 23 September 2024

PUBLISHED 24 October 2024

## CITATION

Wilayat S, Fazil P, Khan JA, Zada A, Ali Shah MI,  
Al-Anazi A, Shah NS, Han C and Ateeq M (2024)  
Degradation of malachite green by UV/H<sub>2</sub>O<sub>2</sub>  
and UV/H<sub>2</sub>O<sub>2</sub>/Fe<sup>2+</sup> processes: kinetics  
and mechanism.  
*Front. Chem.* 12:1467438.  
doi: 10.3389/fchem.2024.1467438

## COPYRIGHT

© 2024 Wilayat, Fazil, Khan, Zada, Ali Shah, Al-Anazi, Shah, Han and Ateeq. This is an open-access article distributed under the terms of the [Creative Commons Attribution License \(CC BY\)](https://creativecommons.org/licenses/by/4.0/). The use, distribution or reproduction in other forums is permitted, provided the original author(s) and the copyright owner(s) are credited and that the original publication in this journal is cited, in accordance with accepted academic practice. No use, distribution or reproduction is permitted which does not comply with these terms.

# Degradation of malachite green by UV/H<sub>2</sub>O<sub>2</sub> and UV/H<sub>2</sub>O<sub>2</sub>/Fe<sup>2+</sup> processes: kinetics and mechanism

Sumaira Wilayat<sup>1</sup>, Perveen Fazil<sup>2</sup>, Javed Ali Khan<sup>1\*</sup>, Amir Zada<sup>1,3</sup>, Muhammad Ishaq Ali Shah<sup>1</sup>, Abdulaziz Al-Anazi<sup>4</sup>, Noor S. Shah<sup>5</sup>, Changseok Han<sup>6,7</sup> and Muhammad Ateeq<sup>1\*</sup>

<sup>1</sup>Department of Chemistry, Abdul Wali Khan University Mardan, Mardan, Khyber Pakhtunkhwa, Pakistan, <sup>2</sup>Department of Chemistry, University of Karachi, Karachi, Pakistan, <sup>3</sup>UNESCO-UNISA Africa Chair in Nanosciences and Nanotechnology, College of Graduate Studies, University of South Africa, Muckleneuk Ridge, Pretoria, South Africa, <sup>4</sup>Department of Chemical Engineering, College of Engineering, King Saud University, Riyadh, Saudi Arabia, <sup>5</sup>Department of Chemistry, COMSATS University Islamabad, Abbottabad, Pakistan, <sup>6</sup>Program in Environmental and Polymer Engineering, Graduate School of INHA University, Incheon, Republic of Korea, <sup>7</sup>Department of Environmental Engineering, INHA University, Incheon, Republic of Korea

This work investigated the photochemical degradation of malachite green (MG), a cationic triphenylmethane dye used as a coloring agent, fungicide, and antiseptic. UV photolysis was ineffective in the removal of MG as only 12.35% degradation of MG (10 mg/L) was achieved after 60 min of irradiation. In contrast, 100.00% degradation of MG (10 mg/L) was observed after 60 min of irradiation in the presence of 10 mM H<sub>2</sub>O<sub>2</sub> by UV/H<sub>2</sub>O<sub>2</sub> at pH 6.0. Similarly, complete removal (100.00%) of MG was observed at 30 min of the reaction time by UV/H<sub>2</sub>O<sub>2</sub>/Fe<sup>2+</sup> employing [MG]<sub>0</sub> = 10 mg/L, [H<sub>2</sub>O<sub>2</sub>]<sub>0</sub> = 10 mM, [Fe<sup>2+</sup>]<sub>0</sub> = 2.5 mg/L, and [pH]<sub>0</sub> = 3.0. For the UV/H<sub>2</sub>O<sub>2</sub> process, the degradation efficiency was higher at pH 6.0 than at pH 3.0 as the *k*<sub>obs</sub> values were 0.0873 and 0.0690 min<sup>-1</sup>, respectively. However, UV/H<sub>2</sub>O<sub>2</sub>/Fe<sup>2+</sup> showed higher reactivity at pH 3.0 than at pH 6.0. Chloride and nitrate ions slightly inhibited the removal efficiency of MG by both UV/H<sub>2</sub>O<sub>2</sub> and UV/H<sub>2</sub>O<sub>2</sub>/Fe<sup>2+</sup> processes. Moreover, three degradation products (DPs) of MG, (i) 4-dimethylamino-benzophenone (DABP), (ii) 4-amino-benzophenone (ABP), and (iii) 4-dimethylamino-phenol (DAP), were identified by GC-MS during the UV/H<sub>2</sub>O<sub>2</sub> treatment. These DPs were found to demonstrate higher aquatic toxicity than the parent MG, suggesting that researchers should focus on the removal of target pollutants as well as their DPs. Nevertheless, the results of this study indicate that both UV/H<sub>2</sub>O<sub>2</sub> and UV/H<sub>2</sub>O<sub>2</sub>/Fe<sup>2+</sup> processes could be implemented to alleviate the harmful environmental impacts of dye and textile industries.

## KEYWORDS

malachite green, UV light, hydrogen peroxide, photo-Fenton, degradation mechanism, wastewater treatment

## 1 Introduction

Synthetic dyes are primarily used in the textile, food, and cosmetics industries. These industries frequently discharge a large amount of untreated and partially treated dye effluents, leading to substantial environmental pollution (Slama et al., 2021). These dyes pose significant harm to human beings and other ecosystems. According to available literature, certain synthetic dyes exhibit toxic properties such as dermatologic effects, allergenic, and carcinogenic (Arora, 2014; Tkaczyk et al., 2020). These dyes constitute the largest category of all colorants, with more than 100,000 varieties available commercially worldwide. The global production of synthetic dyes exceeds 1 million tons annually (Tkaczyk et al., 2020). The extensive use of dyes across various fields greatly impacts water sources (Slama et al., 2021; Tkaczyk et al., 2020; Lal et al., 2024). Synthetic dyes are extensively used in the textile, leather, printing, and paper industries, with certain varieties also being applied in the pharmaceutical and cosmetics industries and in food production (Tkaczyk et al., 2020). The large-scale production of dyes and their broad range of applications lead to the generation of large volumes of colored wastewater and various types of post-production wastes. The textile industry accounts for a significant amount of dyes in aquatic environments, with dye losses during dyeing processes ranging from a minimum of 5% to as much as 50%, depending on the type of fabric and dye. As a result, approximately 200 billion liters of colored effluents are produced annually (Kant, 2012). Additionally, the discharge of textile chemicals raises concerns and presents scientific challenges (Kishor et al., 2021). Given their commercial value, the impacts and risks associated with these chemicals have been studied intensively (Katheresan et al., 2018).

Malachite green (MG), a synthetic dye, is commonly used in aquaculture, textile, and food product industries (Sharma et al., 2023). MG poses potential risks to aquatic life, human health, and the environment (Sharma et al., 2023; Gharavi-Nakhjavani et al., 2023). As a result, regulatory bodies worldwide have taken measures to restrict or ban its use (Gopinathan et al., 2015). Therefore, it is essential to efficiently eliminate synthetic organic dyes from (waste) water (Singh and Arora, 2011). In this regard, different methods have been explored. Several physical, biological, and chemical methods have been used for this purpose, including adsorption to substances, chemical precipitation, photochemical and/or chemical degradation (Khan I. et al., 2020), adsorption (Lanjwani et al., 2024), coagulation (Khan I. et al., 2020; Lanjwani et al., 2024), membrane processes (Oladoye et al., 2023), as well as microbial decolorization (Alsukaibi, 2022) or biological degradation (Thao et al., 2023). Traditional methods were insufficient to treat wastewater containing these stable toxins. However, some methods are very effective in the removal/degradation of toxic environmental pollutants (Sivaraman et al., 2022; Mishra et al., 2019), among which advanced oxidation processes (AOPs) are predominant (Garrido-Cardenas et al., 2020; Fast et al., 2017).

AOPs use highly reactive oxidizing species such as  $\bullet\text{OH}$  and  $\text{SO}_4^{\bullet-}$  to remove organic pollutants from water bodies (Khan et al., 2013; Islam et al., 2023; Hu et al., 2022; Sepúlveda et al., 2024). AOPs have the advantages of being environmentally friendly, achieving complete degradation of pollutants (Fast et al., 2017), and being relatively low cost compared to other methods. Additionally, AOPs can be applied on-site, minimizing the need to transport and treat effluents. Different oxidants such as hydrogen peroxide ( $\text{H}_2\text{O}_2$ ),

peroxymonosulfate ( $\text{HSO}_5^-$ ), and persulfate ( $\text{S}_2\text{O}_8^{2-}$ ) are generally used in AOPs as sources of reactive radicals. Among different AOPs, UV/ $\text{H}_2\text{O}_2$  and UV/ $\text{H}_2\text{O}_2/\text{Fe}^{2+}$  processes are commonly used as (waste)water treatment processes (Khan et al., 2014). Both UV/ $\text{H}_2\text{O}_2$  and UV/ $\text{H}_2\text{O}_2/\text{Fe}^{2+}$  processes are based on the formation of highly reactive and non-selective hydroxyl radicals ( $\bullet\text{OH}$ ). The hydroxyl radical ( $\bullet\text{OH}$ ) possesses a standard redox potential ( $E^\circ$ ) of +2.80 V versus the normal hydrogen electrode (NHE). It exhibits a short lifetime ( $t_{1/2} < 1 \mu\text{s}$ ) and high reactivity, making it a powerful oxidant. Moreover, the reactivity of hydroxyl radical is pH-dependent and has a typical reaction rate of  $10^6$  to  $10^{11} \text{ M}^{-1} \text{ s}^{-1}$  with organic compounds. Notably,  $\bullet\text{OH}$  reacts in a non-selective manner, engaging in various reactions including electron transfer, addition, and abstraction of hydrogen, impacting their reactivity and potential applications in pollutant removal and environmental remediation (Oh et al., 2016).

This study explores the efficacy of MG degradation by UV, UV/ $\text{H}_2\text{O}_2$ , and UV/ $\text{H}_2\text{O}_2/\text{Fe}^{2+}$  processes. The effect of different  $\text{H}_2\text{O}_2$ , MG, and  $\text{Fe}^{2+}$  concentrations and pH conditions on the removal efficiency of MG was evaluated. Moreover, the impact of nitrate and chloride ions was also investigated. In addition, the degradation products (DPs) of MG were identified, and potential degradation pathways were proposed. Finally, the toxicity of the identified DPs and MG was determined using the Ecological Structure Activity Relationship (ECOSAR) Program.

## 2 Experimental

### 2.1 Chemicals and reagents

Malachite green hydrochloride ( $\text{C}_{23}\text{H}_{25}\text{N}_2\text{Cl}$ , molar mass = 364.911 g/mol), hydrochloric acid (HCl, 37.0%), sulfuric acid ( $\text{H}_2\text{SO}_4$ , 95.0%–98.0%), sodium hydroxide (NaOH,  $\geq 97.0\%$ ), potassium chloride (KOH,  $\geq 85.0\%$ ), and sodium nitrate ( $\text{NaNO}_3$ ,  $\geq 99.0\%$ ) were purchased from Sigma-Aldrich. Hydrogen peroxide ( $\text{H}_2\text{O}_2$ , 30% v/v) and ferrous sulfate heptahydrate ( $\text{FeSO}_4 \cdot 7\text{H}_2\text{O}$ ) were supplied by Merck.

### 2.2 Experimental procedures

Experiments were conducted in a photo-reactor consisting of a 100-mL beaker, kept on a magnetic stirrer to continuously mix the reaction solution. The radiation source was a 35-Watt UV lamp (UV-C, wavelength 254 nm, manufactured by Philips, Holland). The concentration of MG in the irradiated solutions was 10 mg/L, if not stated otherwise. Samples of 5 mL from the irradiated solutions were collected at specific time intervals for analysis. Whenever needed, the pH was adjusted with HCl and NaOH.

### 2.3 Analytical methods

A UV-Vis spectrophotometer (PerkinElmer) was used to measure the MG concentration in the treated solutions. The absorbance was recorded at 617 nm. Gas chromatography–mass spectrometry (GC-MS, Agilent

Technologies, 6890 Series) was used to identify the DPs of MG. In GC-MS, the separation was carried out with an HP-5MS capillary column (30 m, 0.25 mm I.D., 0.25  $\mu\text{m}$ ). The oven temperature was programmed as follows: 100°C (1 min) to 180°C at a rate of 20°C min<sup>-1</sup> (3 min) and finally set to 250°C at a rate of 10°C min<sup>-1</sup> (2 min). The temperatures of the injector and MS detector were set at 250°C and 280°C, respectively. The carrier gas was helium (flow rate = 1.0 mL min<sup>-1</sup>). The MS was applied in the EI mode at 70 eV. The DPs were determined at full scan mode ranging from 50 to 550 amu.

Equation 1 was used to determine the degrading efficiency of MG.

$$\text{Degradation efficiency (\%)} = [(C_0 - C_t) / C_0] \times 100, \quad (1)$$

where  $C_0$  represents the starting concentration of MG and  $C_t$  represents the MG concentration at time  $t$ .

## 2.4 Frontier electron densities and point charge calculations

To find the reactive sites/centers in the MG molecule where  $\bullet\text{OH}$  can preferentially attack, the frontier electron densities (FEDs) of the molecular orbitals of MG and point charges of the C and N atoms were calculated using the Gaussian 09 program (An et al., 2015; Rehman et al., 2018). FED calculations were performed for both the highest occupied molecular orbitals (HOMOs) and the lowest unoccupied molecular orbitals (LUMOs). Initially, the geometry of MG was optimized using the HF/3-21 g basis set. Thereafter, the energy calculations for FEDs and point charge determination were performed using the hybrid density functional B3LYP method of the density functional theory (DFT) with the 6-311 g basis set (B3LYP/6-311 g).

## 2.5 Determination of aquatic toxicity

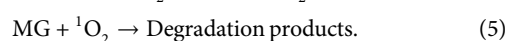
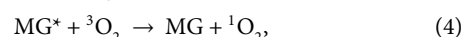
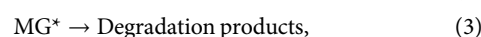
The Ecological Structure Activity Relationship (ECOSAR) program (ECOSAR, 2014) was used to evaluate the acute and chronic toxicities of MG and its DPs. The ECOSAR is an effective tool for predicting the aquatic toxicity of toxic pollutants (Ali et al., 2018). This program evaluates the acute and chronic toxicities of toxic compounds toward fish, daphnia, and green algae. Acute toxicity is evaluated in terms of the LC<sub>50</sub> and EC<sub>50</sub>. LC<sub>50</sub> is the toxicant concentration which could cause the death of 50% fish and 50% daphnia after 96 and 48 h of exposure, respectively. EC<sub>50</sub> is the concentration of the toxicant responsible for 50% growth inhibition of green algae after 96 h of exposure.

# 3 Result and discussion

## 3.1 Direct photolysis of MG

Before investigating the efficiencies of UV/H<sub>2</sub>O<sub>2</sub> and UV/H<sub>2</sub>O<sub>2</sub>/Fe<sup>2+</sup> processes for the degradation of MG, it was studied by direct photolysis (UV only) employing UV-C (254 nm) light. The 254-nm UV-C light photons do not have sufficient amount

of energy to directly split water molecules into reactive species, i.e., hydroxyl radicals ( $\bullet\text{OH}$ ) and hydrated electrons ( $e_{\text{aq}}^-$ ), because only radiation with  $\lambda < 190$  nm can split water to produce  $\bullet\text{OH}$  and  $e_{\text{aq}}^-$  (Gonzalez et al., 2004; Imoberdorf and Mohseni, 2011). Therefore, any degradation of MG at 254 nm radiation can only be attributed to the formation of its excited-state species (MG\*) upon absorption of 254 nm photons (reaction (Equation 2)) (Khan et al., 2014). The excited-state molecules can either undergo direct degradation (reaction (Equation 3)) or may lead to the formation of reactive oxygen species (singlet oxygen,  $^1\text{O}_2$ ) (reaction (Equation 4)) which then attack the MG molecules and cause their degradation (reaction (Equation 5)) (Chen et al., 2008).

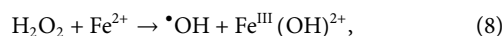
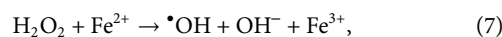
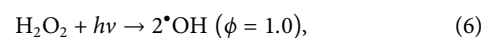


In this study, only 12.35% degradation of MG (10 mg/L) was achieved by direct photolysis at pH 6.0 after 60 min of irradiation. At pH 3.0 and 11.0, a slight decrease in degradation from 12.35% to 10.04% and 11.27%, respectively, was observed. The observed pseudo-first-order rate constant ( $k_{\text{obs}}$ ) was 0.0027, 0.0024, and 0.0022 min<sup>-1</sup> at pH 6.0, 3.0, and 11.0, respectively. These results suggest that direct photolysis is not an effective method for the removal of MG from water (Figure 1). These results are in agreement with findings of Modirshahla and Behnajady (2006). Therefore, UV-C was accompanied by H<sub>2</sub>O<sub>2</sub> and H<sub>2</sub>O<sub>2</sub>/Fe<sup>2+</sup> in the following experiments for efficient degradation of MG.

## 3.2 Degradation of MG by UV/H<sub>2</sub>O<sub>2</sub> and UV/H<sub>2</sub>O<sub>2</sub>/Fe<sup>2+</sup> processes

### 3.2.1 Effect of the initial H<sub>2</sub>O<sub>2</sub> concentration

Both UV/H<sub>2</sub>O<sub>2</sub> and UV/H<sub>2</sub>O<sub>2</sub>/Fe<sup>2+</sup> processes are called hydroxyl radical-based AOPs since they result in the formation of  $\bullet\text{OH}$ , as shown in (Equations 6–9) (Khan et al., 2013; Khan et al., 2017; Shah et al., 2015; Jiad and Abbar, 2023).



The reaction (Equation 9) regenerates ferrous ions (catalyst) during the treatment process and thus helps in continuous production of  $\bullet\text{OH}$  in the reaction mixture, thereby degrading the target pollutants until their complete mineralization, as long as the source of  $\bullet\text{OH}$  (i.e., H<sub>2</sub>O<sub>2</sub>) is available in the solution.

In the present study, four different concentrations of H<sub>2</sub>O<sub>2</sub>, i.e., 2, 5, 10, and 20 mM, were tested for their ability to degrade MG by the UV/H<sub>2</sub>O<sub>2</sub> process at pH 6.0 using 10 mg/L MG. The results are depicted in Figure 2. It was observed that a combination of H<sub>2</sub>O<sub>2</sub> with UV has significantly improved the degradation of MG compared to direct photolysis. The degradation of MG was found to be 78.5, 87.8 and 100% at 60 min in presence of 2, 5

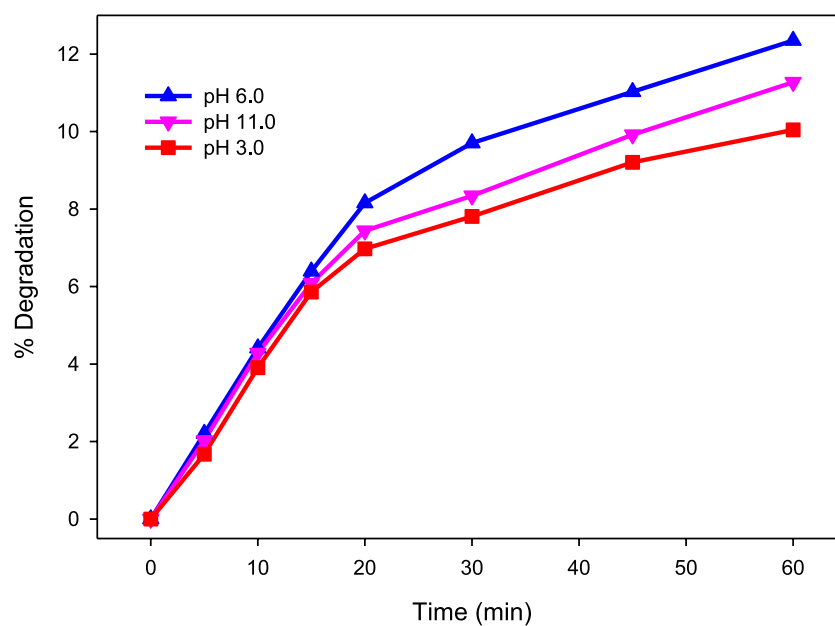


FIGURE 1  
Effect of pH on % degradation of MG by direct photolysis.  $[MG]_0 = 10 \text{ mg/L}$ .

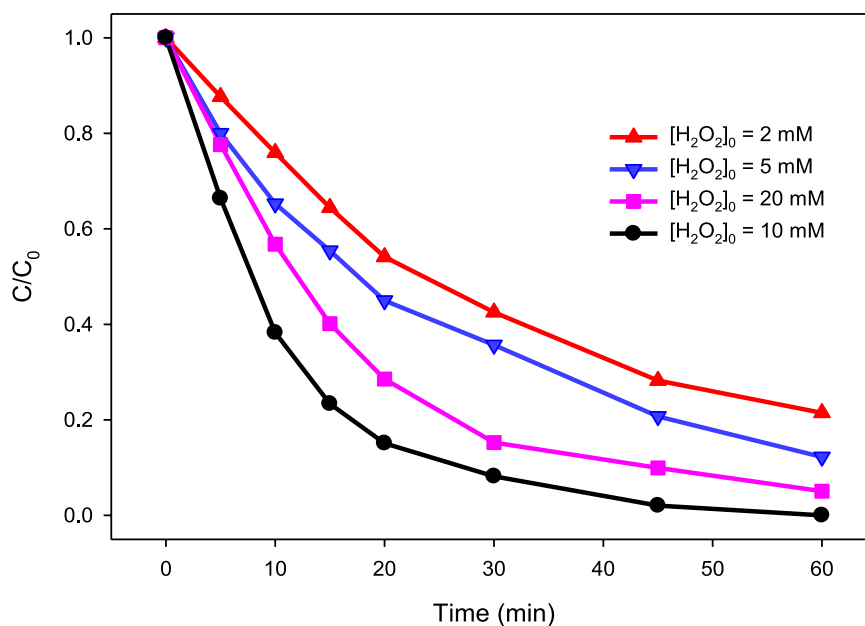
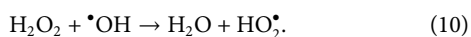


FIGURE 2  
Effect of H<sub>2</sub>O<sub>2</sub> concentration on % degradation of MG in the UV/H<sub>2</sub>O<sub>2</sub> process.  $[H_2O_2]_0 = 2 \text{ mM}$ ,  $5 \text{ mM}$ ,  $10 \text{ mM}$ , and  $20 \text{ mM}$ ,  $[MG]_0 = 10 \text{ mg/L}$ .

and  $10 \text{ mM H}_2\text{O}_2$ , respectively, compared to  $12.35\%$  in direct photolysis. This increase in % degradation was due to the generation of  $\bullet\text{OH}$  in the UV/H<sub>2</sub>O<sub>2</sub> process (reaction (Equation 6)). Since  $\bullet\text{OH}$  radicals are highly reactive and non-selective species, they reacted fast with MG, resulting in its degradation. As the concentration of H<sub>2</sub>O<sub>2</sub> increases in the reaction solution, a larger pool of  $\bullet\text{OH}$  is expected to be produced, thereby enhancing the

degradation process. However, a further increase in H<sub>2</sub>O<sub>2</sub> concentration to  $20 \text{ mM}$  was found to have a detrimental effect on the degradation efficiency as only  $94.9\%$  degradation of MG was observed at the H<sub>2</sub>O<sub>2</sub> concentration of  $20 \text{ mM}$ . The negative impact of higher H<sub>2</sub>O<sub>2</sub> concentration on the degradation efficiency of MG was due to the scavenging effect of H<sub>2</sub>O<sub>2</sub> for  $\bullet\text{OH}$  (Equation 10) (Khan et al., 2013; Modirshahla and Behnajady, 2006; Khan J. A.

et al., 2020; Wei et al., 2020; Rauf et al., 2016). Since this scavenging effect is predominant at higher  $\text{H}_2\text{O}_2$  concentration, a relatively lesser degradation of MG was observed at higher  $\text{H}_2\text{O}_2$  concentration (20 mM) than the optimum value (10 mM). The  $\text{HO}_2^\bullet$  has been reported to be less reactive as compared to  $^\bullet\text{OH}$  and hence do not contribute much toward MG degradation (Modirshahla and Behnajady, 2006; Hameed and Lee, 2009). The  $k_{\text{obs}}$  was calculated to be 0.0271, 0.0355, 0.0873, and 0.0529  $\text{min}^{-1}$  at 2.0, 5.0, 10.0, and 20.0 mM  $\text{H}_2\text{O}_2$ , respectively. Therefore, it is crucial to optimize the  $\text{H}_2\text{O}_2$  concentration to achieve the best result in pollutant removal in  $\text{H}_2\text{O}_2$ -assisted AOPs.



In case of UV/ $\text{H}_2\text{O}_2$ / $\text{Fe}^{2+}$ , the same initial concentrations of  $\text{H}_2\text{O}_2$  were studied as in the case of the UV/ $\text{H}_2\text{O}_2$  process, i.e., 2, 5, 10, and 20 mM. The initial concentration of MG was 10 mg/L, that of  $\text{Fe}^{2+}$  was 2.5 mg/L, and the pH was 3.0. The purpose of acidic pH, i.e., pH 3, was to keep the photo-Fenton system highly efficient as the catalytic activity of  $\text{Fe}^{2+}$  for  $\text{H}_2\text{O}_2$  activation has been found to be the highest at acidic pH values (Khan et al., 2013; Hameed and Lee, 2009; Nasuha et al., 2021). At an initial  $\text{H}_2\text{O}_2$  concentration of 2, 5, 10, and 20 mM, the degradation efficiency was found to be 71.21, 83.31, 95.61%, and 84.77%, respectively, at 20 min (Figure 3). Similarly, the  $k_{\text{obs}}$  values at 2, 5, 10, and 20 mM  $\text{H}_2\text{O}_2$  were found to be 0.0695, 0.0957, 0.1499, and 0.1014  $\text{min}^{-1}$ , respectively. This trend is similar to that found in the UV/ $\text{H}_2\text{O}_2$  process. Thus, it can be suggested that the role of  $\text{H}_2\text{O}_2$  is similar in both UV/ $\text{H}_2\text{O}_2$  and UV/ $\text{H}_2\text{O}_2$ / $\text{Fe}^{2+}$  processes, i.e., initially increasing the level of  $^\bullet\text{OH}$  up to a certain optimum concentration of  $\text{H}_2\text{O}_2$  (10 mM in this case) through reactions Equations 6–9 and then decreasing the level of  $^\bullet\text{OH}$  via the scavenging process (reaction Equation 10)).

### 3.2.2 Effect of initial MG concentration

To analyze how varying concentrations of MG influence its degradation efficiency by UV/ $\text{H}_2\text{O}_2$  and UV/ $\text{H}_2\text{O}_2$ / $\text{Fe}^{2+}$  processes, a series of experiments were conducted at initial concentration of 2.5, 5, 10, and 20 mg/L of  $[\text{MG}]_0$ . For the UV/ $\text{H}_2\text{O}_2$  process, the degradation efficiency was 100.00, 96.98, 84.91%, and 69.43% at 20 min of reaction time when  $[\text{MG}]_0 = 2.5, 5, 10,$  and 20 mg/L of MG, respectively, while applying  $[\text{H}_2\text{O}_2]_0 = 10$  mM and pH = 6.0 (Figure 4). The degradation of MG followed pseudo-first-order kinetics, with the observed pseudo-first-order rate constant ( $k_{\text{obs}}$ ) of 0.1541, 0.1274, 0.0873, and 0.0524  $\text{min}^{-1}$  at  $[\text{MG}]_0 = 2.5, 5, 10,$  and 20 mg/L, respectively.

For the UV/ $\text{H}_2\text{O}_2$ / $\text{Fe}^{2+}$  process, the degradation efficiency was 100, 89.92, 77.99, and 69.49% at 10 min of treatment when the initial MG concentration was 2.5, 5, 10, and 20 mg/L, respectively (Figure 5), employing  $[\text{Fe}^{2+}]_0 = 2.5$  mg/L,  $[\text{H}_2\text{O}_2]_0 = 10$  mM, and pH = 3.0. The  $k_{\text{obs}}$  values were found to be 0.3884, 0.2333, 0.1565, and 0.1180  $\text{min}^{-1}$  for  $[\text{MG}]_0 = 2.5, 5, 10,$  and 20 mg/L, respectively.

These results clearly indicated that as the concentration of MG increases, the degradation efficiency decreases for both of the UV/ $\text{H}_2\text{O}_2$  and UV/ $\text{H}_2\text{O}_2$ / $\text{Fe}^{2+}$  processes. Since both these processes rely on the same reactive species, i.e.,  $^\bullet\text{OH}$ , and the source of  $^\bullet\text{OH}$  (i.e.,  $\text{H}_2\text{O}_2$ ) is also the same in both processes, the reasons for the reduced degradation efficiency at higher MG concentration are also the same. The reduced degradation efficiency at a higher dye concentration is the solution's elevated absorbance. This is particularly relevant because MG has a significant absorbance below 300 nm, which is the same range where  $\text{H}_2\text{O}_2$  absorbs (Navarro et al., 2019). It means that the color produced by the MG dye acts as a filter for UV light and thereby reduces the penetration of light into the reaction mixture.

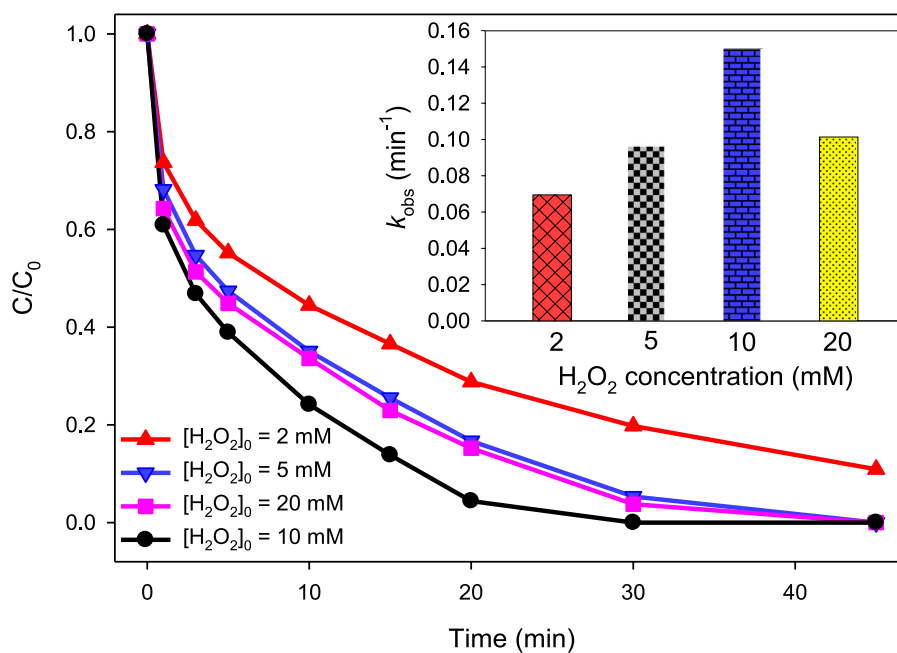


FIGURE 3 Effect of  $\text{H}_2\text{O}_2$  concentration on the UV/ $\text{H}_2\text{O}_2$ / $\text{Fe}^{2+}$  process.  $[\text{Fe}^{2+}]_0 = 2.5$  mg/L,  $[\text{MG}]_0 = 10$  mg/L,  $[\text{H}_2\text{O}_2]_0 = 2, 5, 10,$  and 20 mM, pH 3.0. The inset indicates the  $k_{\text{obs}}$  values at studied  $\text{H}_2\text{O}_2$  concentrations.

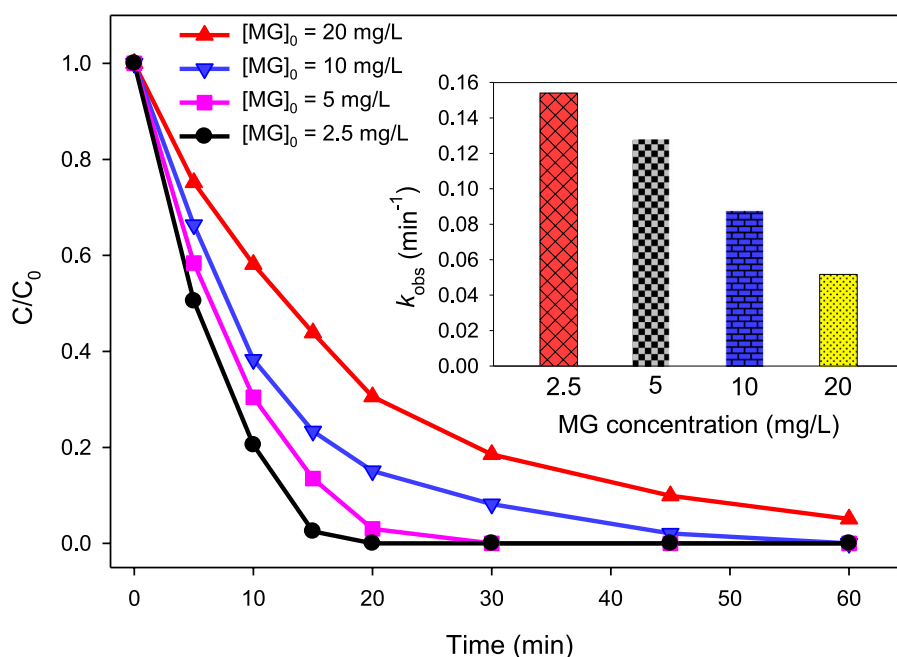


FIGURE 4 Effect of MG concentration on % degradation of malachite green in the UV/H<sub>2</sub>O<sub>2</sub> process. [H<sub>2</sub>O<sub>2</sub>]<sub>0</sub> = 10 mM, [MG]<sub>0</sub> = 2.5 mg/L, 5 mg/L, 10 mg/L, and 20 mg/L. The inset indicates the  $k_{obs}$  values at different MG concentrations.

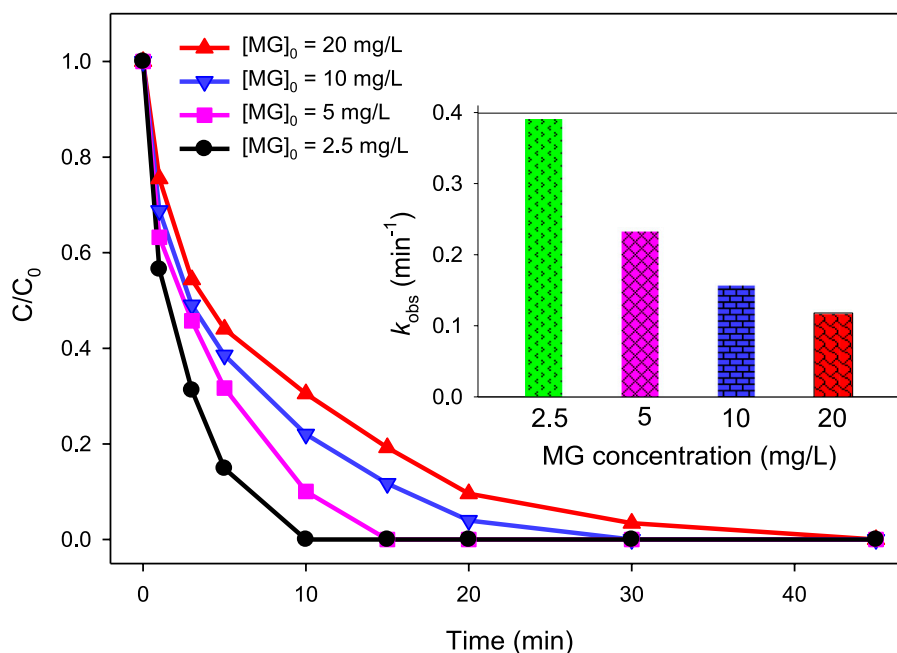


FIGURE 5 Effect of MG concentration on the UV/H<sub>2</sub>O<sub>2</sub>/Fe<sup>2+</sup> process. [Fe<sup>2+</sup>]<sub>0</sub> = 2.5 mg/L, [MG]<sub>0</sub> = 2.5 mg/L, 5 mg/L, 10 mg/L, and 20 mg/L. [H<sub>2</sub>O<sub>2</sub>]<sub>0</sub> = 10 mM, pH 3.0. The inset indicates the  $k_{obs}$  values at different MG concentrations.

As a result, at higher MG concentration, fewer photons are available to interact with the H<sub>2</sub>O<sub>2</sub> molecule. Consequently, there will be lesser production of hydroxyl radicals, which are responsible for the degradation of dye molecules. By the same

reason, the rate of regeneration of catalyst (Fe<sup>2+</sup>) via reaction (9) also decreases at higher MG concentration. Consequently, the rate of H<sub>2</sub>O<sub>2</sub> activation by Fe<sup>2+</sup> to produce <sup>•</sup>OH via reaction (7) also decreases at higher MG concentration. Thus, the filter out of



the UV light by the dye color resulted in reduced  $\cdot\text{OH}$  formation, which ultimately led to the lower degradation efficiency of MG in both UV/ $\text{H}_2\text{O}_2$  and UV/ $\text{H}_2\text{O}_2/\text{Fe}^{2+}$  processes at higher MG concentration. Another possible reason of the lower degradation efficiency at higher MG concentration is the enhanced level of intermediate (degradation products of MG) molecules produced at higher MG concentration. As a result, the competition between MG and intermediate molecules for  $\cdot\text{OH}$  increases, and there are greater chances for  $\cdot\text{OH}$  to react with intermediate molecules rather than MG molecules when the level of intermediate molecules enhances at higher MG concentration, which led to lower degradation efficiency of MG.

Though the % degradation decreases with increase in MG concentration, the rate of degradation (the number of molecules undergo degradation per unit time) increases with increase in MG concentration. At higher MG concentration, a higher number of the dye molecules are exposed to reactive radicals, and hence, the chances of collisions between  $\cdot\text{OH}$  and MG molecules increase, which led to the higher degradation rate of MG (Khan et al., 2013; Rehman et al., 2018; Galindo et al., 2001). As a result, the rate of MG degradation was calculated to be 0.103, 0.217, 0.562, and 0.745 mg/L/min at 2.5, 5, 10, and 20 mg/L MG concentration, respectively, at 10 min of reaction time for the UV/ $\text{H}_2\text{O}_2$  process. Similarly, for the UV/ $\text{H}_2\text{O}_2/\text{Fe}^{2+}$  process at 5 min of reaction time, the rate of degradation of MG was found to be 0.426, 0.770, 1.130, and 2.191 mg/L/min at 2.5, 5, 10, and 20 mg/L MG concentration, respectively.

Of note, % degradation is a relative term that refers to the number of molecules undergoing degradation related to the total number of molecules in the system. This relative quantity decreases

with an increase in the target compound concentration. On the other hand, the rate of degradation is an absolute term which represents the actual number of molecules undergo degradation in the given specified time. It is not related to the total number of molecules. This absolute quantity increases with an increase in the target compound concentration.

### 3.2.3 Effect of $\text{Fe}^{2+}$ concentration on MG degradation by the UV/ $\text{H}_2\text{O}_2/\text{Fe}^{2+}$ process

To investigate the effect of different concentrations of  $\text{Fe}^{2+}$  on the degradation of MG by the UV/ $\text{H}_2\text{O}_2/\text{Fe}^{2+}$  process, a series of experiments were conducted using different initial concentrations of  $\text{Fe}^{2+}$  (i.e., 0.5, 1, 2.5, and 5 mg/L). Other conditions were kept constant at  $[\text{H}_2\text{O}_2]_0 = 10$  mM,  $[\text{MG}]_0 = 10$  mg/L, and pH = 3.0. The obtained results are depicted in Figure 6. The results indicated that the degradation efficiency increases with increasing the initial concentration of  $\text{Fe}^{2+}$  ( $[\text{Fe}^{2+}]_0$ ). At  $[\text{Fe}^{2+}]_0$  of 0.5, 1.0, 2.5, and 5.0 mg/L, the degradation efficiencies were 71.17, 80.25, 88.31, and 96.05% at 15 min, respectively. Similarly, the values of  $k_{\text{obs}}$  were found to be 0.093, 0.113, 0.1565, and 0.2204  $\text{min}^{-1}$  at  $[\text{Fe}^{2+}]_0 = 0.5, 1.0, 2.5,$  and 5.0 mg/L, respectively. The increase in degradation of MG with an increase in  $[\text{Fe}^{2+}]_0$  is due to the presence of Fenton-like reaction (Equation 7).  $\text{Fe}^{2+}$  triggers the activation of  $\text{H}_2\text{O}_2$ , leading to the formation of  $\cdot\text{OH}$  via an electron transfer process where electrons move from  $\text{Fe}^{2+}$  to  $\text{H}_2\text{O}_2$  (De Laat and Gallard, 1999). Therefore, as the  $[\text{Fe}^{2+}]_0$  increases, the rate of  $\cdot\text{OH}$  formation increases, which subsequently led to higher degradation efficiency of MG.

Further insight into the relationship between  $k_{\text{obs}}$  and  $[\text{Fe}^{2+}]_0$  showed that the increase in  $k_{\text{obs}}$  with increase in  $[\text{Fe}^{2+}]_0$  is not linear

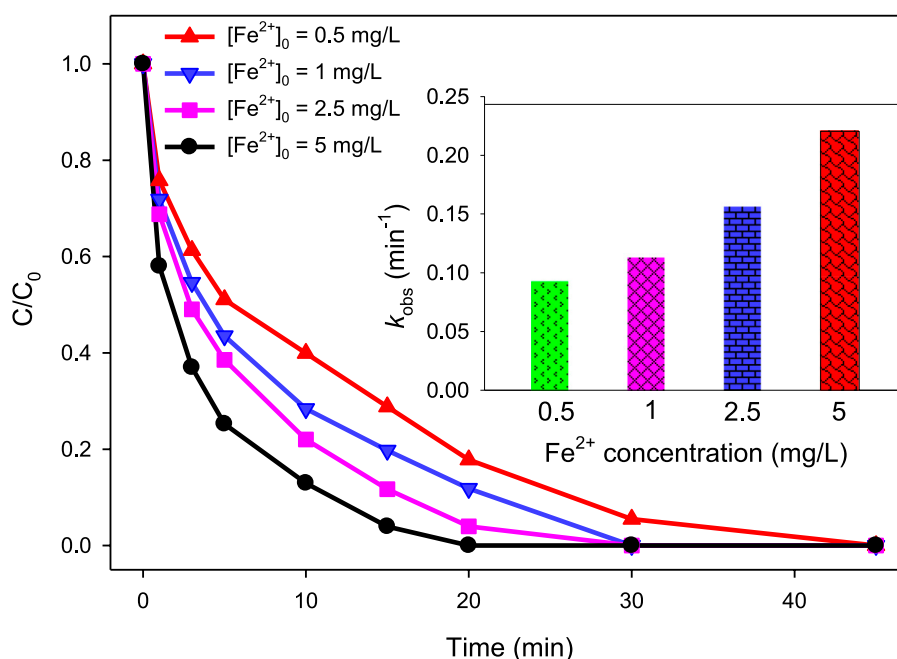
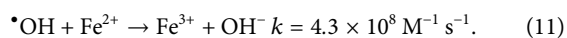


FIGURE 6 Effect of  $\text{Fe}^{2+}$  concentration on % degradation of MG in the UV/ $\text{H}_2\text{O}_2/\text{Fe}^{2+}$  process.  $[\text{MG}]_0 = 10$  mg/L,  $[\text{H}_2\text{O}_2]_0 = 10$  mM, pH 3.0. The inset indicates the relationship between  $k_{\text{obs}}$  and  $\text{Fe}^{2+}$  concentration.

(Figure 6 inset). This non-linear relation is due to the  $\cdot\text{OH}$  scavenging effect of  $\text{Fe}^{2+}$  at a substantially higher concentration (Equation 11) (Hameed and Lee, 2009; Chen and Pignatello, 1997; Joseph et al., 2000).



### 3.2.4 Effect of pH

pH is a crucial factor that significantly impacts the effectiveness of AOPs by influencing the generation of  $\cdot\text{OH}$  and is consistently taken into account for the optimization of water treatment processes. To study the effect of pH on the

degradation of MG by  $\text{UV}/\text{H}_2\text{O}_2$  and  $\text{UV}/\text{H}_2\text{O}_2/\text{Fe}^{2+}$  processes and determine the optimal pH of the reaction mixture, experiments were carried out at pH = 3.0 and 6.0. For  $\text{UV}/\text{H}_2\text{O}_2$ , the concentrations of MG and  $\text{H}_2\text{O}_2$  were kept constant at 10 mg/L and 10 mM, respectively. For  $\text{UV}/\text{H}_2\text{O}_2/\text{Fe}^{2+}$ , the same concentrations of MG and  $\text{H}_2\text{O}_2$  were used in addition to  $[\text{Fe}^{2+}]_0 = 2.5 \text{ mg/L}$ . The results indicated that the degradation of MG was influenced by the pH of the solution (Figure 7). For the  $\text{UV}/\text{H}_2\text{O}_2$  process, the degradation efficiency was higher at pH 6.0 compared to pH 3.0. Specifically, 91.82% MG degradation was observed at pH 6.0 compared to 84.35% at pH 3.0 after 30 min of irradiation. The  $k_{\text{obs}}$  value decreased from 0.0873 to

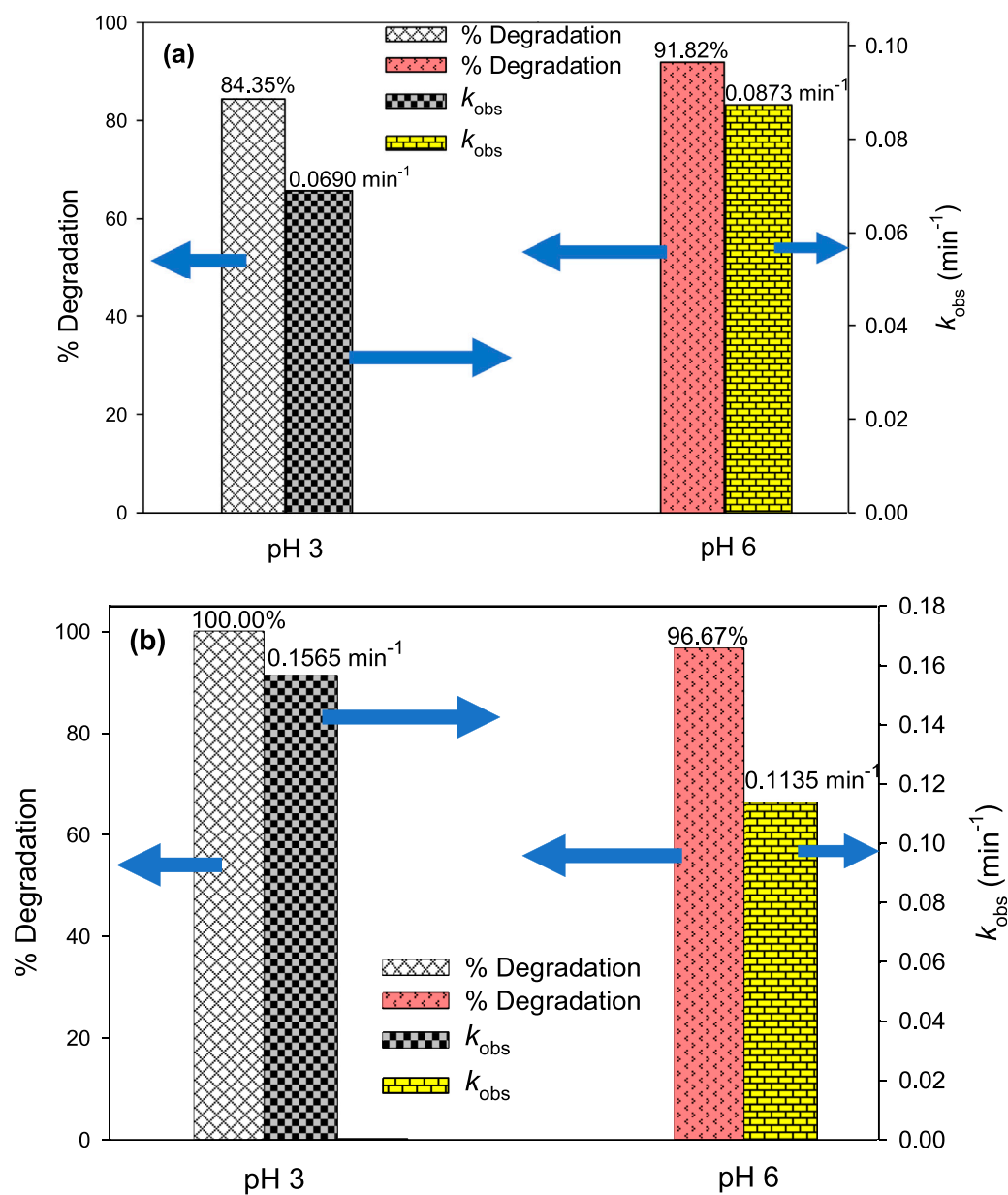


FIGURE 7 Effect of pH on % degradation and  $k_{\text{obs}}$  of MG by  $\text{UV}/\text{H}_2\text{O}_2$  (A) and  $\text{UV}/\text{H}_2\text{O}_2/\text{Fe}^{2+}$  (B). Experimental conditions:  $[\text{MG}]_0 = 10 \text{ mg/L}$ ,  $[\text{H}_2\text{O}_2]_0 = 10 \text{ mM}$ , and  $[\text{Fe}^{2+}]_0 = 2.5 \text{ mg/L}$ .



TABLE 1 Comparison of MG removal by UV/H<sub>2</sub>O<sub>2</sub> and UV/H<sub>2</sub>O<sub>2</sub>/Fe<sup>2+</sup> processes studied in this work and those reported by other researchers.

Method	Concentration of malachite green (mg/L)	[H <sub>2</sub> O <sub>2</sub> ] <sub>0</sub>	[Fe <sup>2+</sup> ] <sub>0</sub>	pH	Time (min)	Degradation (%)	Reference
UV/H <sub>2</sub> O <sub>2</sub>	10	10 mM	----	6.0	60	100	This study
UV/H <sub>2</sub> O <sub>2</sub> /Fe <sup>2+</sup>	10	10 mM	2.5 mg/L	3.0	30	100	This study
UV/H <sub>2</sub> O <sub>2</sub>	10	300 mg/L	----	----	≈25–30	100	Modirshahla and Behnajady (2006)
UV/H <sub>2</sub> O <sub>2</sub>	25	1.5 mL of 33% H <sub>2</sub> O <sub>2</sub> /250 mL	----	5.6	50	96	Dar et al. (2023)
UV/H <sub>2</sub> O <sub>2</sub> /Fe <sup>2+</sup>	25	1.5 mL of 33% H <sub>2</sub> O <sub>2</sub> /250 mL	----	----	40	100	Dar et al. (2023)
UV/H <sub>2</sub> O <sub>2</sub>	100	12 mM	----	3.0	60	95	Ghime et al. (2019)
UV/H <sub>2</sub> O <sub>2</sub> /Fe <sup>2+</sup>	100	12 mM	60 ppm	3.0	60	98	Ghime et al. (2019)

TABLE 2 Comparison of different AOPs for the degradation of malachite green.

Method	Malachite green (mg/L)	Experimental condition	Time (min)	Degradation (%)	Reference
UV/H <sub>2</sub> O <sub>2</sub>	10	10 mM H <sub>2</sub> O <sub>2</sub> , pH 6.0	60	100	This study
UV/H <sub>2</sub> O <sub>2</sub> /Fe <sup>2+</sup>	10	10 mM H <sub>2</sub> O <sub>2</sub> , 2.5 mg/L Fe <sup>2+</sup> , pH 3.0		100	This study
TiO <sub>2</sub> photocatalysis	100	0.6 g/L TiO <sub>2</sub> , UV light (32-W lamp)	60	95	Ghime et al. (2019)
TiO <sub>2</sub> photocatalysis	10	0.5 g/L TiO <sub>2</sub> , UV-A light (9 W lamp)	40	100	Berberidou et al. (2007)
Sonolysis (under argon)	10	135 W ultrasound power, argon atmosphere	120	100	Berberidou et al. (2007)
Chemical oxidation with ozone (O <sub>3</sub> )	36.49	Ozone (0.5 g/h), pH 3.0, 5.0, and 7.0	110	96.74 at pH 3.0, 80.5 at pH 5.0, and 50.1 at pH 7.0	Mirila et al. (2018)
Electrochemical oxidation	20	I = 32 mA.cm <sup>-2</sup> , pH = 3, [Na <sub>2</sub> SO <sub>4</sub> ] = 0.1 mol/L, boron-doped diamond (BDD)	60	98	Guenfoud et al. (2014)
Kissiris/Fe <sub>3</sub> O <sub>4</sub> /TiO <sub>2</sub> with the glucose oxidase (GOx) enzyme	20	Initial glucose concentration = 20 mM, pH 5.5, temp. = 40°C, catalyst = 2 g	120	99	Elhami et al. (2015)

0.0690 min<sup>-1</sup> as the pH changed from 6.0 to 3.0 (Figure 7A). However, 100% degradation of MG was achieved after 60 min of treatment at both pH 3.0 and 6.0. Hence, the UV/H<sub>2</sub>O<sub>2</sub> process shows higher degradation efficiency at pH 6.0 as compared to acidic pH. Iron-based processes such as Fenton and photo-Fenton are AOPs that demonstrate a strong pH dependence where acidity has been found as a favorable condition for the degradation of target compounds (Khan et al., 2013; Chan and Chu, 2003; Yong et al., 2015). Unlike the UV/H<sub>2</sub>O<sub>2</sub> process, UV/H<sub>2</sub>O<sub>2</sub>/Fe<sup>2+</sup> showed higher removal efficiency at pH 3.0 than at pH 6.0. The degradation of MG was found to be 100.00% and 96.67% after 30 min of treatment at pH 3.0 and pH 6.0, corresponding to *k*<sub>obs</sub> of 0.1565 and 0.1135 min<sup>-1</sup>, respectively (Figure 7B). A comparable pattern was noticed by Hassan et al. (2023) and Khan et al. (2013). Fe<sup>2+</sup> has been found to have higher catalytic activity at acidic conditions for H<sub>2</sub>O<sub>2</sub> activation to

generate •OH (Equation 7) (Khan et al., 2013; Chan and Chu, 2003). As the pH increases, iron undergoes precipitation in the form of Fe(OH)<sub>3</sub> and hence, Fe<sup>2+</sup> was not available to activate H<sub>2</sub>O<sub>2</sub> for •OH generation, thereby hindering the degradation efficiency of MG at pH 6.0 (Deb et al., 2023).

To better understand the efficiencies of the AOPs studied in this work in comparison with the similar AOPs reported previously on the degradation of MG, please refer to Table 1. Moreover, Table 2 summarizes the comparison of the efficiencies of different AOPs applied for the treatment of MG. Both these tables provide important information for enriching the existing knowledge on the removal of dyes by various AOPs.

### 3.2.5 Effect of chloride and nitrate ions

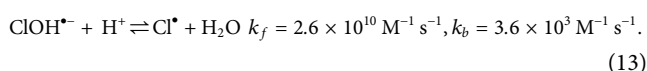
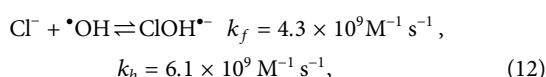
To investigate the effect of common inorganic ions on the degradation efficiency of MG by UV/H<sub>2</sub>O<sub>2</sub> and UV/H<sub>2</sub>O<sub>2</sub>/Fe<sup>2+</sup>

TABLE 3 Effect of chloride and nitrate ions on % degradation and  $k_{obs}$  of MG by UV/H<sub>2</sub>O<sub>2</sub> and UV/H<sub>2</sub>O<sub>2</sub>/Fe<sup>2+</sup> processes. Experimental conditions: [MG]<sub>0</sub> = 10 mg/L, [H<sub>2</sub>O<sub>2</sub>]<sub>0</sub> = 10 mM, [Fe<sup>2+</sup>]<sub>0</sub> = 2.5 mg/L. pH was 6.0 for UV/H<sub>2</sub>O<sub>2</sub> and 3.0 for UV/H<sub>2</sub>O<sub>2</sub>/Fe<sup>2+</sup>.

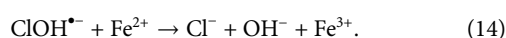
Anion	UV/H <sub>2</sub> O <sub>2</sub>		UV/H <sub>2</sub> O <sub>2</sub> /Fe <sup>2+</sup>	
	% degradation at 60 min of treatment	$k_{obs}$ (min <sup>-1</sup> )	% degradation at 20 min of treatment	$k_{obs}$ (min <sup>-1</sup> )
No scavenger	100.00	0.0873	96.00	0.1565
Chloride ion (5 mM)	84.10	0.0415	78.18	0.0817
Nitrate ion (5 mM)	91.95	0.0502	85.46	0.1016

processes, the degradation of MG was studied in the presence of chloride (Cl<sup>-</sup>) and nitrate ions (NO<sub>3</sub><sup>-</sup>) used as representative inorganic ions. It was found that both Cl<sup>-</sup> and NO<sub>3</sub><sup>-</sup> slightly reduced the degradation efficiency of MG (Table 3). For the UV/H<sub>2</sub>O<sub>2</sub> process, the degradation of MG decreased from 100.0% to 84.1% and 91.95% at 60 min of treatment in the presence of 5 mM each of Cl<sup>-</sup> and NO<sub>3</sub><sup>-</sup>, respectively, employing [MG]<sub>0</sub> = 10 mg/L [H<sub>2</sub>O<sub>2</sub>]<sub>0</sub> = 10 mM, and [pH]<sub>0</sub> = 6. The  $k_{obs}$  was found to be 0.0873, 0.0415, and 0.0502 min<sup>-1</sup> in the presence of no scavenger, Cl<sup>-</sup> and NO<sub>3</sub><sup>-</sup>, respectively (Table 3). Similarly, for the UV/H<sub>2</sub>O<sub>2</sub>/Fe<sup>2+</sup> process, the degradation of MG decreased from 96.0% to 78.2% and 85.5% at 20 min of treatment in the presence of 5 mM each of Cl<sup>-</sup> and NO<sub>3</sub><sup>-</sup>, respectively, employing [MG]<sub>0</sub> = 10 mg/L, [H<sub>2</sub>O<sub>2</sub>]<sub>0</sub> = 10 mM, [Fe<sup>2+</sup>]<sub>0</sub> = 2.5 mg/L, and [pH]<sub>0</sub> = 3. The  $k_{obs}$  of MG by UV/H<sub>2</sub>O<sub>2</sub>/Fe<sup>2+</sup> was found to be 0.1565, 0.0817, and 0.1016 min<sup>-1</sup> in the presence of no scavenger, Cl<sup>-</sup> and NO<sub>3</sub><sup>-</sup>, respectively (Table 3).

The reduction in the degradation efficiency of MG by Cl<sup>-</sup> in both processes, i.e., UV/H<sub>2</sub>O<sub>2</sub> and UV/H<sub>2</sub>O<sub>2</sub>/Fe<sup>2+</sup>, could possibly be attributed to the scavenging effect of Cl<sup>-</sup> for •OH. This is because the main reactive species in both of these processes is •OH, as confirmed by the methanol scavenging test (data not shown). Chloride ions quench •OH effectively in accordance with reactions Equation 12, 13 (Muruganandham and Swaminathan, 2004; Alshamsi et al., 2007).



The slight decrease in the removal efficiency of MG by Cl<sup>-</sup> may possibly be due to the reversibility of reaction Equation 12, which re-produces the •OH via backward reaction with a little higher rate constant ( $k_b$ ) than its scavenging via forward reaction ( $k_f$ ). Moreover, the presence of Fe<sup>2+</sup> in UV/H<sub>2</sub>O<sub>2</sub>/Fe<sup>2+</sup>, could also potentially contribute to the lower removal efficiency of MG by Cl<sup>-</sup> (reaction (Equation 14)) (Ali et al., 2018; Malik and Saha, 2003).



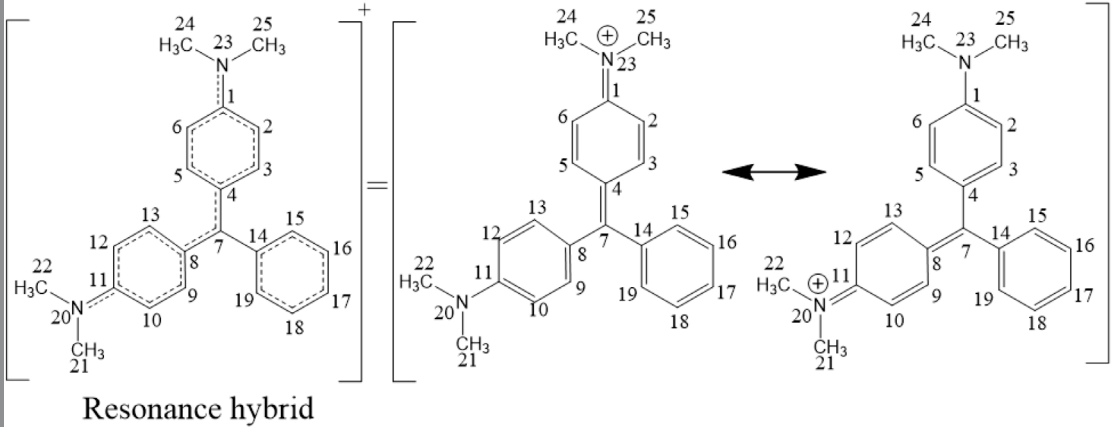
Nitrate ions (NO<sub>3</sub><sup>-</sup>) were found to have a less retarding effect than Cl<sup>-</sup> on the degradation of MG by both UV/H<sub>2</sub>O<sub>2</sub> and UV/H<sub>2</sub>O<sub>2</sub>/Fe<sup>2+</sup> processes. This could possibly be due to the low reactivity of NO<sub>3</sub><sup>-</sup> with •OH (Rehman et al., 2018).

### 3.3 Identification of degradation products and possible degradation pathways

The DPs of MG produced during UV/H<sub>2</sub>O<sub>2</sub> treatment were identified by GC-MS. Prior to discussing the experimentally detected DPs of MG, it is highly useful to find the potential reactive sites of MG where •OH could initially attack via addition or hydrogen abstraction reactions. For this purpose, the density functional theory (DFT) calculations were performed using the HF/3-21 g basis set for optimization and B3LYP/6-311 g basis set for energy calculations. The DFT calculations were performed using the Gaussian 09 program to find out the FEDs and point charges of the MG atoms to predict the positions in the MG molecule where •OH can easily undergo addition or hydrogen abstraction reactions. The calculated values of FEDs and point charges of the MG are given in Table 4. It has been reported that atoms having larger values of (FED<sup>2</sup><sub>HOMO</sub> + FED<sup>2</sup><sub>LUMO</sub>) are more likely to be attacked by the •OH via addition reaction/pathway (An et al., 2015). On the other hand, •OH could preferably abstract hydrogen from atoms having more positive charge. Based on this information, the •OH could initially react with C7 atom via the addition reaction due to its large (FED<sup>2</sup><sub>HOMO</sub> + FED<sup>2</sup><sub>LUMO</sub>) value (An et al., 2015; Rehman et al., 2018). The next preferable sites of •OH addition reactions could be the N20 and N23 atoms followed by the C4 and C8 atoms. The highest point charge values are possessed by C1 and C11 atoms due to their attachment with the electronegative N atoms. However, both of these C atoms bear no hydrogen atom to be abstracted by •OH. Similarly, the carbon atoms bearing the next higher value of point charge, i.e., C7, also lack hydrogen atoms to be abstracted by •OH. The same is the case with C14, which has the next higher value of point charge. Therefore, the possible hydrogen abstraction sites are proposed to be C3 and C9 as well as C5 and C13, which have the lowest negative values (i.e., relatively large values) of point charge among the atoms bearing hydrogen atoms.

In the present work, three DPs of MG were identified, namely: (a) 4-dimethylamino-benzophenone (DABP), (b) 4-amino-benzophenone (ABP), and (c) 4-dimethylamino-phenol (DAP) (Scheme 1). The hydroxyl radical could possibly attack the central carbon atom of MG, leading to the formation of a hydroxylated reactive cationic radical (MG-OH)—not detected in the present study but is supposed to be a tentative degradation product based on the DFT calculations

TABLE 4 Frontier electron densities and point charges of MG atoms calculated by the Gaussian 09 program.



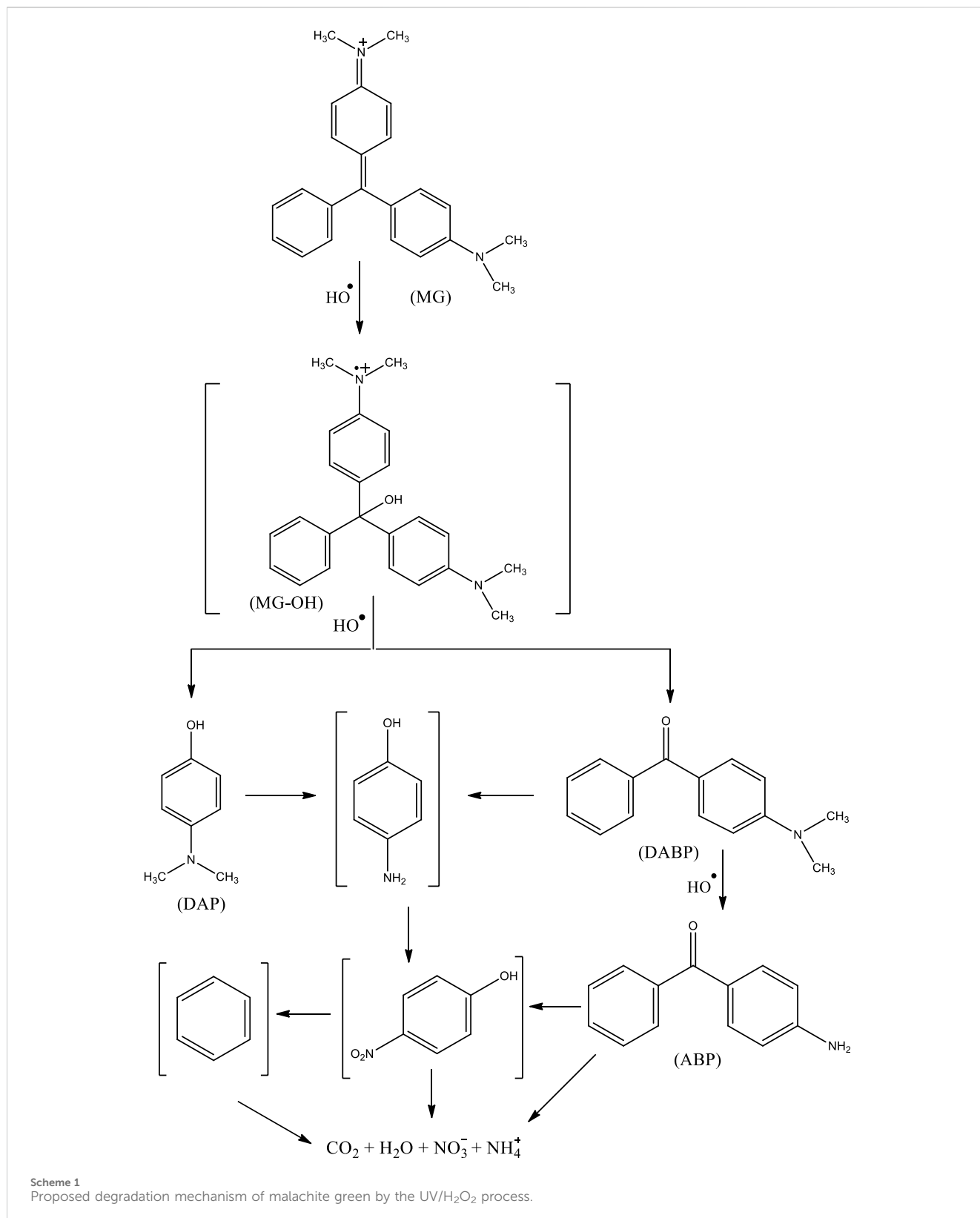
Atom	FED <sup>2</sup> <sub>HOMO</sub> + FED <sup>2</sup> <sub>LUMO</sub>	Point charge	Atom	FED <sup>2</sup> <sub>HOMO</sub> + FED <sup>2</sup> <sub>LUMO</sub>	Point charge
C1	0.0590	0.23732	C14	0.0236	-0.09591
C2	0.0452	-0.25008	C15	0.0408	-0.16964
C3	0.0578	-0.12135	C16	0.0066	-0.18682
C4	0.0774	-0.13303	C17	0.0288	-0.15825
C5	0.0567	-0.12959	C18	0.0066	-0.18681
C6	0.0480	-0.25203	C19	0.0408	-0.16964
C7	0.2168	0.15527	C20	0.1724	-0.36351
C8	0.0774	-0.13303	C21	0.0019	-0.36622
C9	0.0578	-0.12135	C22	0.0019	-0.36616
C10	0.0452	-0.25008	N23	0.1723	-0.36351
C11	0.0590	0.23732	C24	0.0019	-0.36616
C12	0.0479	-0.25203	C25	0.0019	-0.36622
C13	0.0567	-0.12960			

(Berberidou et al., 2007). The subsequent demethylation and further oxidation by  $\bullet\text{OH}$  finally led to the formation of DAP and DABP (Berberidou et al., 2007). The demethylation of DABP—a common reaction of MG—could then lead to the formation of ABP (Berberidou et al., 2007). The mentioned three DPs have also been detected by other researchers while studying the degradation of MG by AOPs (Berberidou et al., 2007; Milano et al., 1995; Xie et al., 2001; Chen et al., 2002; Ju et al., 2009). Moreover, it has been previously reported that the cleavage of benzophenone generally leads to the formation of benzene and benzaldehyde (Berberidou et al., 2007). The formation of amino-benzene from MG and then its conversion to nitro-benzene by  $\bullet\text{OH}$  have also been reported (Berberidou et al., 2007). The attack of  $\bullet\text{OH}$  on lower-molecular weight aromatic DPs such as amino-benzene, nitro-benzene, benzaldehyde, and benzene further leads to the formation of lower-molecular weight organic acids, which subsequently lead to the formation of  $\text{CO}_2$ ,  $\text{H}_2\text{O}$ , nitrate, nitrite, and/or ammonium ions (Xie et al., 2001; Ju et al., 2009). The present study suggests that treatment

of MG-containing water by HR-AOPs not only leads to its complete degradation but also leads to its complete mineralization—albeit slowly.

### 3.4 Toxicity evaluation

The ultimate goal of a water treatment technology is to achieve clean and pure water, i.e., toxicant-free water. To check whether the toxicity of the treating mixture reduces during the degradation of MG or not, the aquatic toxicity of the detected DPs toward fish, daphnia, and green algae was determined using the ECOSAR program (Rehman et al., 2023; Iqbal et al., 2024a; Iqbal et al., 2024b; Khan et al., 2023) (Table 5). Surprisingly, all the three detected DPs were found to have higher toxicity (both acute and chronic) than the parent MG. Therefore, it can be concluded that the researchers should not just focus on the removal of target compound while dealing with the removal of dyes. Rather, the toxicity of the treated solution



should be determined before, during, and after the treatment in order to ensure the reduction in toxicity of the treated solution. Moreover, the treatment time should be prolonged such that the

treatment technology not only degrades/removes the target pollutant but also the DPs, i.e., until complete mineralization is achieved.

TABLE 5 Aquatic toxicity of malachite green and its identified DPs (unit = mg L<sup>-1</sup>).

Compound	Acute toxicity			Chronic toxicity		
	Fish (LC <sub>50</sub> )	Daphnia (LC <sub>50</sub> )	Green algae (EC <sub>50</sub> )	Fish (ChV)	Daphnia (ChV)	Green algae (ChV)
MG	3,230	1,640	774	277	118	158
DABP	12.0	7.67	9.48	1.35	1.05	3.26
ABP	15.1	1.79	4.48	0.138	0.022	1.11
DAP	442	236	137	40.2	19.4	31.2

## 4 Conclusion

The present study investigated the degradation of MG by UV/H<sub>2</sub>O<sub>2</sub> and UV/H<sub>2</sub>O<sub>2</sub>/Fe<sup>2+</sup> processes. MG was found to be resistant toward direct photolysis as only 12.35% MG degradation was achieved by direct photolysis at pH 6.0 after 60 min of treatment. However, the combination of H<sub>2</sub>O<sub>2</sub> with UV light accelerated the degradation of MG, achieving 100% degradation of MG at 10 mM H<sub>2</sub>O<sub>2</sub> concentration when treated for 60 min, suggesting the higher reactivity of MG with •OH. Further enhancement in the degradation efficiency of MG by UV/H<sub>2</sub>O<sub>2</sub> was observed by adding Fe<sup>2+</sup> ion—an effective catalyst for H<sub>2</sub>O<sub>2</sub> activation—as 100% degradation of MG was observed at [Fe<sup>2+</sup>]<sub>0</sub> = 2.5 mg/L and 30 min of treatment. The higher concentration of MG was found to have a detrimental effect on its degradation by both UV/H<sub>2</sub>O<sub>2</sub> and UV/H<sub>2</sub>O<sub>2</sub>/Fe<sup>2+</sup> processes. However, increasing concentrations of H<sub>2</sub>O<sub>2</sub> and Fe<sup>2+</sup> were found to have a positive effect on MG degradation. For the UV/H<sub>2</sub>O<sub>2</sub> process, a higher removal efficiency of MG was observed at pH 6.0 as compared to at pH 3.0. Nitrate (NO<sub>3</sub><sup>-</sup>) and chloride ions (Cl<sup>-</sup>) have negatively impacted the MG degradation by both UV/H<sub>2</sub>O<sub>2</sub> and UV/H<sub>2</sub>O<sub>2</sub>/Fe<sup>2+</sup> processes. However, NO<sub>3</sub><sup>-</sup> showed less retarding effect than Cl<sup>-</sup>, possibly due to the lower reactivity of NO<sub>3</sub><sup>-</sup> with •OH than that of Cl<sup>-</sup>. Based on the GC-MS analysis, three degradation products (DPs) of MG were identified, namely: (a) 4-dimethylamino-benzophenone (DABP), (b) 4-amino-benzophenone (ABP), and (c) 4-dimethylamino-phenol (DAP). The computational aquatic toxicity study toward three aquatic organisms (fish, daphnia, and green algae) showed that all of the detected DPs are more toxic than MG. The present study revealed that MG can effectively be degraded by hydroxyl radical-based AOPs; however, researchers should also ensure the complete removal of its DPs so that the toxicity of the treated water may not increase due to the formation of toxic DPs.

## Data availability statement

The original contributions presented in the study are included in the article; further inquiries can be directed to the corresponding authors.

## Author contributions

SW: conceptualization, data curation, formal analysis, investigation, methodology, and writing—original draft. PF: conceptualization, data curation, formal analysis, methodology, and writing—original draft. JK: conceptualization, funding acquisition, investigation,

supervision, and writing—review and editing. AZ: software, validation, and writing—review and editing. MA: conceptualization and writing—review and editing. AA-A: funding acquisition, validation, and writing—review and editing. NS: conceptualization and writing—review and editing. CH: software, validation, and writing—review and editing. MA: conceptualization, funding acquisition, project administration, supervision, validation, and writing—review and editing.

## Funding

The author(s) declare financial support was received for the research, authorship, and/or publication of this article. The authors highly acknowledge the financial support from Abdul Wali Khan University Mardan, Pakistan, through Research Innovation Fund (RIF). CH acknowledges the support of the National Research Foundation of Korea (NRF) grant funded by the Korean government (MSIT) (Nos. 2021R1A2C1093183 and 2021R1A4A1032746). The authors also gratefully acknowledge the Researchers Supporting Project (number RSPD2024R534), King Saud University, Riyadh, Saudi Arabia.

## Acknowledgments

The authors highly acknowledge the financial support from Abdul Wali Khan University Mardan, Pakistan, through Research Innovation Fund (RIF). CH acknowledges the support of the National Research Foundation of Korea (NRF) grant funded by the Korean government (MSIT) (Nos. 2021R1A2C1093183 and 2021R1A4A1032746). The authors also gratefully acknowledge the Researchers Supporting Project (number RSPD2024R534), King Saud University, Riyadh, Saudi Arabia.

## Conflict of interest

The authors declare that the research was conducted in the absence of any commercial or financial relationships that could be construed as a potential conflict of interest.

The author(s) declared that they were an editorial board member of Frontiers, at the time of submission. This had no impact on the peer review process and the final decision.



## Publisher's note

All claims expressed in this article are solely those of the authors and do not necessarily represent those of their affiliated

organizations, or those of the publisher, the editors, and the reviewers. Any product that may be evaluated in this article, or claim that may be made by its manufacturer, is not guaranteed or endorsed by the publisher.

## References

- Ali, F., Khan, J. A., Shah, N. S., Sayed, M., and Khan, H. M. (2018). Carbamazepine degradation by UV and UV-assisted AOPs: kinetics, mechanism and toxicity investigations. *Process Saf. Environ. Prot.* 117, 307–314. doi:10.1016/j.psep.2018.05.004
- Alshamsi, F. A., Albadwawi, A. S., Alnuaimi, M. M., Rauf, M. A., and Ashraf, S. S. (2007). Comparative efficiencies of the degradation of Crystal Violet using UV/hydrogen peroxide and Fenton's reagent. *Dyes Pigm.* 74, 283–287. doi:10.1016/j.dyepig.2006.02.016
- Alsukaibi, A. K. (2022). Various approaches for the detoxification of toxic dyes in wastewater. *Processes* 10 (10), 1968. doi:10.3390/pr10101968
- An, T., An, J., Gao, Y., Li, G., Fang, H., and Song, W. (2015). Photocatalytic degradation and mineralization mechanism and toxicity assessment of antiviral drug acyclovir: experimental and theoretical studies. *Appl. Catal. B Environ.* 164, 279–287. doi:10.1016/j.apcatb.2014.09.009
- Arora, S. (2014). Textile dyes: its impact on environment and its treatment. *J. Bioremed. Biodeg.* 5 (3), 1. doi:10.4172/2155-6199.1000e146
- Berberidou, C., Poullos, I., Xekoukoulotakis, N. P., and Mantzavinos, D. (2007). Sonolytic, photocatalytic and sonophotocatalytic degradation of malachite green in aqueous solutions. *Appl. Catal. B Environ.* 74, 63–72. doi:10.1016/j.apcatb.2007.01.013
- Chan, K., and Chu, W. (2003). Modeling the reaction kinetics of Fenton's process on the removal of atrazine. *Chemosphere* 51, 305–311. doi:10.1016/s0045-6535(02)00812-3
- Chen, F., He, J., Zhao, J., and Yu, J. C. (2002). Photo-Fenton degradation of malachite green catalyzed by aromatic compounds under visible light irradiation. *New J. Chem.* 26, 336–341. doi:10.1039/b107404k
- Chen, R., and Pignatello, J. (1997). Role of quinone intermediates as electron shuttles in Fenton and photoassisted Fenton oxidations of aromatic compounds. *Environ. Sci. Technol.* 31, 2399–2406. doi:10.1021/es9610646
- Chen, Y., Hu, C., Qu, J., Yang, M., and Chemistry, P. A. (2008). Photodegradation of tetracycline and formation of reactive oxygen species in aqueous tetracycline solution under simulated sunlight irradiation. *J. Photochem. Photobiol. A Chem.* 197, 81–87. doi:10.1016/j.jphotochem.2007.12.007
- Dar, A., Anwar, J., and Munir, A. (2023). Photocatalytic degradation of malachite green dye with UV/H<sub>2</sub>O<sub>2</sub> system in presence of transition metal ions. *J. Chem. Soc. Pak.* 45 (6), 302. doi:10.52568/001284/jcsp/45.04.2023
- Deb, A., Rumky, J., and Sillanpää, M. (2023). "Fenton, photo-Fenton, and electro-Fenton systems for micropollutant treatment processes," in *Advanced oxidation processes for micropollutant remediation*. Editors M. Khalid, Y. Park, R. R. Karri, and R. Walvekar (Boca Raton, FL: CRC press, Taylor & Francis group), 157–185. doi:10.1201/9781003247913-8
- De Laat, J., and Gallard, H. (1999). Catalytic decomposition of hydrogen peroxide by Fe (III) in homogeneous aqueous solution: mechanism and kinetic modeling. *Environ. Sci. Technol.* 33, 2726–2732. doi:10.1021/es981171v
- Elhami, V., Karimi, A., and Aghbolaghy, M. (2015). Preparation of heterogeneous bio-Fenton catalyst for decolorization of Malachite Green. *J. Taiwan Inst. Chem. E.* 56, 154–159. doi:10.1016/j.jtice.2015.05.006
- Fast, S. A., Gude, V. G., Truax, D. D., Martin, J., and Magbanua, B. S. (2017). A critical evaluation of advanced oxidation processes for emerging contaminants removal. *Environ. Process.* 4, 283–302. doi:10.1007/s40710-017-0207-1
- Galindo, C., Jacques, P., Kalt, A., and P. A. (2001). Photochemical and photocatalytic degradation of an indigoid dye: a case study of acid blue 74 (AB74). *J. Photochem. Photobiol. A Chem.* 141, 47–56. doi:10.1016/s1010-6030(01)00435-x
- Garrido-Cardenas, J. A., Esteban-García, B., Agüera, A., Sánchez-Pérez, J. A., and Manzano-Agugliaro, F. (2020). Wastewater treatment by advanced oxidation process and their worldwide research trends. *Int. J. Environ. Res. Public Health* 17 (1), 170. doi:10.3390/ijerph17010170
- Gharavi-Nakhjavani, M. S., Niazi, A., Hosseini, H., Aminzare, M., Dizaji, R., Tajdar-Oranj, B., et al. (2023). Malachite green and leucomalachite green in fish: a global systematic review and meta-analysis. *Environ. Sci. Pollut. Res.* 30 (17), 48911–48927. doi:10.1007/s11356-023-26372-z
- Ghime, D., Goru, P., Ojha, S., and Ghosh, P. (2019). Oxidative decolorization of a malachite green oxalate dye through the photochemical advanced oxidation processes. *Glob. Nest J.* 21 (2), 195. doi:10.30955/gnj.003000
- Gonzalez, M. G., Oliveros, E., Wörner, M., and Braun, A. M. (2004). Vacuum-ultraviolet photolysis of aqueous reaction systems. *J. Photochem. Photobiol. C. Photochem. Rev.* 5, 225–246. doi:10.1016/j.jphotochemrev.2004.10.002
- Gopinathan, R., Kanhere, J., and Banerjee, J. (2015). Effect of malachite green toxicity on non-target soil organisms. *Chemosphere* 120, 637–644. doi:10.1016/j.chemosphere.2014.09.043
- Guenfoud, F., Mokhtari, M., and Akrouf, H. (2014). Electrochemical degradation of malachite green with BDD electrodes: effect of electrochemical parameters. *Diam. Relat. Mater.* 46, 8–14. doi:10.1016/j.diamond.2014.04.003
- Hameed, B., and Lee, T. (2009). Degradation of malachite green in aqueous solution by Fenton process. *J. Hazard. Mater.* 164, 468–472. doi:10.1016/j.jhazmat.2008.08.018
- Hassan, A. F., Mustafa, A., Esmail, G., and Awad, A. (2023). Adsorption and photo-fenton degradation of methylene blue using nanomagnetite/potassium carrageenan biocomposite beads. *Arab. J. Sci. Eng.* 48, 353–373. doi:10.1007/s13369-022-07075-y
- Hu, J., Chen, S., and Liang, X. (2022). Heterogeneous catalytic oxidation for the degradation of aniline in aqueous solution by persulfate activated with CuFe<sub>2</sub>O<sub>4</sub>/activated carbon catalyst. *ChemistrySelect* 7, e202201241. doi:10.1002/slct.202201241
- Imoberdorf, G., and Mohseni, M. (2011). Degradation of natural organic matter in surface water using vacuum-UV irradiation. *J. Hazard. Mater.* 186, 240–246. doi:10.1016/j.jhazmat.2010.10.118
- Iqbal, J., Shah, N. S., Ali Khan, J., Ibrahim, A., Masood Pirzada, B., Naushad, M., et al. (2024a). Visible light driven ZnFe<sub>2</sub>O<sub>4</sub> for the degradation of oxytetracycline in the presence of HSO<sub>5</sub><sup>-</sup> at semi-pilot scale and additional H<sub>2</sub> production. *Chem. Eng. J.* 498, 155402. doi:10.1016/j.cej.2024.155402
- Iqbal, J., Shah, N. S., Ali Khan, J., Naushad, M., Boczkaj, G., Jamil, F., et al. (2024b). Pharmaceuticals wastewater treatment via different advanced oxidation processes: reaction mechanism, operational factors, toxicities, and cost evaluation – a review. *Sep. Purif. Technol.* 347, 127458. doi:10.1016/j.seppur.2024.127458
- Islam, M., Kumar, S., Saxena, N., and Nafees, A. (2023). Photocatalytic degradation of dyes present in industrial effluents: a review. *ChemistrySelect* 8, e202301048. doi:10.1002/slct.202301048
- Jiad, M. M., and Abbar, A. H. (2023). Efficient wastewater treatment in petroleum refineries: hybrid electro-Fenton and photocatalysis (UV/ZnO) process. *Chem. Eng. Res. Des.* 200, 431–444. doi:10.1016/j.cherd.2023.10.050
- Joseph, J. M., Destaillets, H., Hung, H.-M., and Hoffmann, M. R. (2000). The sonochemical degradation of azobenzene and related azo dyes: rate enhancements via Fenton's reactions. *J. Phys. Chem. A* 104, 301–307. doi:10.1021/jp992354m
- Ju, Y., Yang, S., Ding, Y., Sun, C., Gu, C., He, Z., et al. (2009). Microwave-enhanced H<sub>2</sub>O<sub>2</sub>-based process for treating aqueous malachite green solutions: intermediates and degradation mechanism. *J. Hazard. Mater.* 171, 123–132. doi:10.1016/j.jhazmat.2009.05.120
- Kant, R. (2012). Textile dyeing industry an environmental hazard. *Nat. Sci.* 4 (1), 22–26. doi:10.4236/ns.2012.41004
- Katheresan, V., Kansedo, J., and Lau, S. Y. (2018). Efficiency of various recent wastewater dye removal methods: a review. *J. Environ. Chem. Eng.* 6 (4), 4676–4697. doi:10.1016/j.jece.2018.06.060
- Khan, I., Saeed, K., Ali, N., Khan, I., Zhang, B., and Sadiq, M. (2020a). Heterogeneous photodegradation of industrial dyes: an insight to different mechanisms and rate affecting parameters. *J. Environ. Chem. Eng.* 8 (5), 104364. doi:10.1016/j.jece.2020.104364
- Khan, J. A., He, X., Khan, H. M., Shah, N. S., and Dionysiou, D. D. (2013). Oxidative degradation of atrazine in aqueous solution by UV/H<sub>2</sub>O<sub>2</sub>/Fe<sup>2+</sup>, UV/S<sub>2</sub>O<sub>8</sub><sup>2-</sup>/Fe<sup>2+</sup> and UV/HSO<sub>5</sub><sup>-</sup>/Fe<sup>2+</sup> processes: a comparative study. *Chem. Eng. J.* 218, 376–383. doi:10.1016/j.cej.2012.12.055
- Khan, J. A., He, X., Shah, N. S., Khan, H. M., Hapeshi, E., Fatta-Kassinos, D., et al. (2014). Kinetic and mechanism investigation on the photochemical degradation of atrazine with activated H<sub>2</sub>O<sub>2</sub>, S<sub>2</sub>O<sub>8</sub><sup>2-</sup> and HSO<sub>5</sub><sup>-</sup>. *Chem. Eng. J.* 252, 393–403. doi:10.1016/j.cej.2014.04.104
- Khan, J. A., He, X., Shah, N. S., Sayed, M., Khan, H. M., and Dionysiou, D. D. (2017). Degradation kinetics and mechanism of desethyl-atrazine and desisopropyl-atrazine in water with •OH and SO<sub>4</sub><sup>-</sup> based-AOPs. *Chem. Eng. J.* 325, 485–494. doi:10.1016/j.cej.2017.05.011
- Khan, J. A., Sayed, M., Shah, N. S., Khan, S., Khan, A. A., Sultan, M., et al. (2023). Synthesis of N-doped TiO<sub>2</sub> nanoparticles with enhanced photocatalytic activity for 2,4-dichlorophenol degradation and H<sub>2</sub> production. *J. Environ. Chem. Eng.* 11, 111308. doi:10.1016/j.jece.2023.111308
- Khan, J. A., Sayed, M., Shah, N. S., Khan, S., Zhang, Y., Boczkaj, G., et al. (2020b). Synthesis of eosin modified TiO<sub>2</sub> film with co-exposed {001} and {101} facets for

- photocatalytic degradation of para-aminobenzoic acid and solar H<sub>2</sub> production. *Appl. Catal. B Environ.* 265, 118557. doi:10.1016/j.apcatb.2019.118557
- Kishor, R., Purchase, D., Saratale, G. D., Saratale, R. G., Ferreira, L. F. R., Bilal, M., et al. (2021). Ecotoxicological and health concerns of persistent coloring pollutants of textile industry wastewater and treatment approaches for environmental safety. *J. Environ. Chem. Eng.* 9 (2), 105012. doi:10.1016/j.jece.2020.105012
- Lal, R., Gour, T., Dave, N., Singh, N., Yadav, J., Khan, A., et al. (2024). Green route to fabrication of Semal-ZnO nanoparticles for efficient solar-driven catalysis of noxious dyes in diverse aquatic environments. *Front. Chem.* 12, 1370667. doi:10.3389/fchem.2024.1370667
- Lanjwani, M. F., Tuzen, M., Khuawar, M. Y., and Saleh, T. A. (2024). Trends in photocatalytic degradation of organic dye pollutants using nanoparticles: a review. *Inorg. Chem. Commun.* 159, 111613. doi:10.1016/j.inoche.2023.111613
- Malik, P. K., and Saha, S. K. (2003). Oxidation of direct dyes with hydrogen peroxide using ferrous ion as catalyst. *Sep. Purif. Technol.* 31, 241–250. doi:10.1016/s1383-5866(02)00200-9
- Milano, J. C., Lose-Berdot, P., and Vernet, J. L. (1995). Photooxydation du Vert de Malachite en Milieu Aqueux en Presence de Peroxyde D'Hydrogene: Cinetique et Mecanisme Photooxydation of Malachite Green in Aqueous Medium in the Presence of Hydrogen Peroxide: Kinetic and Mechanism. *Environ. Technol.* 16, 329–341. doi:10.1080/09593331608616275
- Mirila, D. C., Pirvan, M. Ş., Platon, N., Georgescu, A. M., Zichil, V., and Nistor, I. D. (2018). Total mineralization of malachite green dye by advanced oxidation processes. *Acta Chem. Iasi* 26, 263–280. doi:10.2478/achi-2018-0017
- Mishra, S., Chowdhary, P., and Bharagava, R. N. (2019). "Conventional methods for the removal of industrial pollutants, their merits and demerits," in *Emerging and eco-friendly approaches for waste management*. Editors R. N. Bharagava and P. Chowdhary (Springer), 1–31.
- Modirshahla, N., and Behnajady, M. (2006). Photooxidative degradation of Malachite Green (MG) by UV/H<sub>2</sub>O<sub>2</sub>: influence of operational parameters and kinetic modeling. *Dyes Pigm* 70, 54–59. doi:10.1016/j.dyepig.2005.04.012
- Muruganandham, M., and Swaminathan, M. (2004). Photochemical oxidation of reactive azo dye with UV-H<sub>2</sub>O<sub>2</sub> process. *Dyes Pigm* 62, 269–275. doi:10.1016/j.dyepig.2003.12.006
- Nasuha, N., Hameed, B., and Okoye, P. (2021). Dark-Fenton oxidative degradation of methylene blue and acid blue 29 dyes using sulfuric acid-activated slag of the steel-making process. *J. Environ. Chem. Eng.* 9, 104831. doi:10.1016/j.jece.2020.104831
- Navarro, P., Zapata, J. P., Gotor, G., Gonzalez-Olmos, R., and Gómez-López, V. (2019). Degradation of malachite green by a pulsed light/H<sub>2</sub>O<sub>2</sub> process. *Water Sci. Technol.* 79, 260–269. doi:10.2166/wst.2019.041
- Oh, W. D., Dong, Z., and Lim, T. T. (2016). Generation of sulfate radical through heterogeneous catalysis for organic contaminants removal: current development, challenges and prospects. *Appl. Catal. B Environ.* 194, 169–201. doi:10.1016/j.apcatb.2016.04.003
- Oladoye, P. O., Ajiboye, T. O., Wanyonyi, W. C., Omotola, E. O., and Oladipo, M. E. (2023). Insights into remediation technology for malachite green wastewater treatment. *Water Sci. Technol.* 16 (3), 261–270. doi:10.1016/j.wse.2023.03.002
- Rauf, M. A., Ali, L., Sadig, M. S., Ashraf, S. S., and Hisaindee, S. (2016). Comparative degradation studies of Malachite Green and Thiazole Yellow G and their binary mixture using UV/H<sub>2</sub>O<sub>2</sub>. *Desalin. Water Treat.* 57, 8336–8342. doi:10.1080/19443994.2015.1017745
- Rehman, F., Parveen, N., Iqbal, J., Sayed, M., Shah, N. S., Ansar, S., et al. (2023). Potential degradation of norfloxacin using UV-C/Fe<sup>2+</sup>/peroxides-based oxidative pathways. *J. Photochem. Photobiol. A Chem.* 435, 114305. doi:10.1016/j.jphotochem.2022.114305
- Rehman, F., Sayed, M., Khan, J. A., Shah, N. S., Khan, H. M., and Dionysiou, D. D. (2018). Oxidative removal of brilliant green by UV/S<sub>2</sub>O<sub>8</sub><sup>2-</sup>, UV/HSO<sub>5</sub><sup>-</sup> and UV/H<sub>2</sub>O<sub>2</sub> processes in aqueous media: a comparative study. *J. Hazard. Mater.* 357, 506–514. doi:10.1016/j.jhazmat.2018.06.012
- Sepúlveda, M., Musiał, J., Saldan, I., Chennam, P. K., Rodriguez-Pereira, J., Sopha, H., et al. (2024). Photocatalytic degradation of naproxen using TiO<sub>2</sub> single nanotubes. *Front. Environ. Chem.* 5, 1373320. doi:10.3389/fenvc.2024.1373320
- Shah, N. S., He, X., Khan, J. A., Khan, H. M., Boccelli, D. L., and Dionysiou, D. D. (2015). Comparative studies of various iron-mediated oxidative systems for the photochemical degradation of endosulfan in aqueous solution. *J. Photochem. Photobiol. A Chem.* 306, 80–86. doi:10.1016/j.jphotochem.2015.03.014
- Sharma, J., Sharma, S., and Soni, V. (2023). Toxicity of malachite green on plants and its phytoremediation: a review. *Regional Stud. Mar. Sci.* 62, 102911. doi:10.1016/j.rmsa.2023.102911
- Singh, K., and Arora, S. (2011). Removal of synthetic textile dyes from wastewaters: a critical review on present treatment technologies. *Crit. Rev. Environ. Sci. Technol.* 41, 807–878. doi:10.1080/10643380903218376
- Sivaraman, C., Vijayalakshmi, S., Leonard, E., Sagadevan, S., and Jambulingam, R. (2022). Current developments in the effective removal of environmental pollutants through photocatalytic degradation using nanomaterials. *Catalysts* 12 (5), 544. doi:10.3390/catal12050544
- Slama, H. B., Chenari Bouket, A., Pourhassan, Z., Alenezi, F. N., Silini, A., Cherif-Silini, H., et al. (2021). Diversity of synthetic dyes from textile industries, discharge impacts and treatment methods. *Appl. Sci.* 11 (14), 6255. doi:10.3390/app11146255
- Thao, T. T. P., Nguyen-Thi, M. L., Chung, N. D., Ooi, C. W., Park, S. M., Lan, T. T., et al. (2023). Microbial biodegradation of recalcitrant synthetic dyes from textile-enriched wastewater by *Fusarium oxysporum*. *Chemosphere* 325, 138392. doi:10.1016/j.chemosphere.2023.138392
- Tkaczyk, A., Mitrowska, K., and Posyniak, A. (2020). Synthetic organic dyes as contaminants of the aquatic environment and their implications for ecosystems: a review. *Sci. Total Environ.* 717, 137222. doi:10.1016/j.scitotenv.2020.137222
- Wei, Y., Wang, C., Liu, D., Jiang, L., Chen, X., Li, H., et al. (2020). Photo-catalytic oxidation for pyridine in circumneutral aqueous solution by magnetic Fe-Cu materials activated H<sub>2</sub>O<sub>2</sub>. *Chem. Eng. Res. Des.* 163, 1–11. doi:10.1016/j.cherd.2020.08.007
- Xie, Y., Wu, K., Chen, F., He, J., and Zhao, J. (2001). Investigation of the intermediates formed during the degradation of malachite green in the presence of Fe<sup>2+</sup> and H<sub>2</sub>O<sub>2</sub> under visible irradiation. *Res. Chem. Intermed.* 27, 237–248. doi:10.1163/156856701300356455
- Yong, L., Zhanqi, G., Yuefei, J., Xiaobin, H., Cheng, S., Shaogui, Y., et al. (2015). Photodegradation of malachite green under simulated and natural irradiation: kinetics, products, and pathways. *J. Hazard. Mater.* 285, 127–136. doi:10.1016/j.jhazmat.2014.11.041